JOURNAL OF VIROLOGY, May 2011, p. 4309–4317 Vol. 85, No. 9
0022-538X/11/$12.00 doi:10.1128/JVI.02575-10

Marburg Virus VP40 Antagonizes Interferon Signaling in a Species-Specific Manner▽

Charalampos Valmas and Christopher F. Basler*

Department of Microbiology, Mount Sinai School of Medicine, New York, New York 10029

Received 10 December 2010/Accepted 6 January 2011

Marburgviruses are zoonotic pathogens that cause lethal hemorrhagic fever in humans and nonhuman primates. However, they do not cause lethal disease in immunocompetent mice unless they are adapted to this species. The adaptation process can therefore provide insight into the specific virus-host interactions that determine virulence. In primate cells, the *Lake Victoria marburgvirus* Musoke strain (MARV) VP40 matrix protein antagonizes alpha/beta interferon (IFN-α/β) and IFN-γ signaling by inhibiting the activation of the cellular tyrosine kinase Jak1. Here, VP40 from the Ravn strain (RAVV VP40)—from a distinct Marburg virus clade—is demonstrated to also inhibit IFN signaling in human cells. However, neither MARV nor RAVV VP40 effectively inhibited IFN-signaling in mouse cells, as assessed by assays of the antiviral effects of IFN-α/β and the IFN-α/β-induced phosphorylation of Jak1, STAT1, and STAT2. In contrast, the VP40 from a mouse-adapted RAVV (maRAVV) did inhibit IFN signaling. Effective Jak1 inhibition correlated with the species from which the cells were derived and did not depend upon whether Jak1 was of human or mouse origin. Of the seven amino acid changes that accumulated in VP40 during mouse adaptation, two (V57A and T165A) are sufficient to allow efficient IFN signaling antagonism by RAVV VP40 in mouse cells. The same two changes also confer efficient IFN antagonist function upon MARV VP40 in mouse cells. The mouse-adaptive changes did not affect the budding of RAVV VP40 in mouse cells, suggesting that this second major function of VP40 did not undergo adaptation. These data identify an apparent determinant of RAVV host range and virulence and define specific genetic determinants of this function.

Filoviruses, which include the genera *Marburgvirus* and *Ebolavirus* (EBOV), are causative agents of severe hemorrhagic fevers in humans and nonhuman primates. Human case fatality rates have reached up to 90% in some outbreaks. The genus *Marburgvirus* includes a single species, *Lake Victoria marburgvirus* that is comprised of two lineages; one is represented by a 1987 isolate from Kenya (Marburg Ravn virus [RAVV]), and the other is comprised of multiple strains, including Ozolin, Popp, Musoke (abbreviated as MARV here), and Angola (10, 14, 33).

Filoviruses counteract the innate immune responses of primate hosts, preventing the production of and cellular responses to alpha/beta interferon (IFN-α/β) (1, 28, 29, 40). IFN-α/β and IFN-γ are cytokines that induce in cells an antiviral state and are of particular importance to innate antiviral immunity (3, 36). Binding of IFN-α/β to its receptor results in the tyrosine phosphorylation of the Janus kinases Jak1 and Tyk2, which subsequently phosphorylate the transcription factors STAT1 and STAT2. STAT1 and STAT2 form a heterodimer and associate with the IFN regulatory factor 9 (IRF9), translocate into the nucleus, and activate a set of genes involved in antiviral response (25). The absence of Jak1 leads to lack of STAT activation (11, 21, 30, 44).

Filovirus proteins that antagonize IFN responses have been identified. EBOV VP35 inhibits the production of IFN-α/β by antagonizing the RIG-I signaling pathway (1, 6, 12, 17). EBOV VP24 inhibits cellular responses to IFN-α/β and IFN-γ by interacting with the NPI-1 subfamily of karyopherin α nuclear transport proteins, preventing the nuclear accumulation of tyrosine phosphorylated STAT1 (20, 28, 29). Surprisingly, given the similar genomic organization of EBOVs and Marburg viruses, MARV was demonstrated to block cellular responses to IFNs by a unique mechanism (40). Specifically, while the MARV VP24 protein did not exhibit binding to karyopherin α proteins and did not block IFN signaling, the MARV major matrix protein VP40, which drives viral budding (8, 16, 34, 39), inhibits Jak1-dependent signaling pathways, including the IFN-α/β, IFN-γ, and interleukin-6 pathways (40). For the IFN-α/β pathway, VP40 inhibits activation of Jak1, resulting in the absence of IFN-α/β-induced Jak1, Tyk2, STAT1, and STAT2 tyrosine phosphorylation (40).

The assembly and budding functions of filovirus VP40 proteins are related to their ability to bud from cells, and expression of VP40 proteins results in the release of virus-like particles (VLPs) from the cell surface (13, 15, 16, 23, 32, 39). Implicated in the budding process are short amino acid motifs known as late domains. EBOV VP40 possesses two late domains: a PTAP motif and an overlapping PPXY motif (13, 23). These mediate interaction with host proteins Tsg101, Nedd4, and Rsp5 (13, 35). MARV VP40 possesses a single PPPY motif that allows interaction with Tsg101 (39). However, late domains represent only one component required for efficient budding. For example, Liu et al. have demonstrated the existence of additional conserved motifs (EBOV VP40 $_{96}$LPLGVA$_{101}$ or Marburg virus VP40 $_{84}$LPLGIM$_{89}$) that are also critical for release of VLPs (18).

Because nonadapted filoviruses do not kill adult immunocompetent mice or guinea pigs and because of the need for

* Corresponding author. Mailing address: Department Microbiology, Box 1124, Mount Sinai School of Medicine, 1 Gustave L. Levy Place, New York, NY 10029. Phone: (212) 241-4847. Fax: (212) 534-1684. E-mail: chris.basler@mssm.edu.

▽ Published ahead of print on 16 February 2011.

small animal models of infection, several groups have generated guinea pig- and mouse-adapted Marburg viruses and EBOVs (5, 9, 19, 41–43). These studies have implicated changes in Zaire EBOV NP and VP24 for lethal mouse infection and changes in Zaire EBOV VP24 for lethal guinea pig infection (9, 26, 41). Specific molecular mechanisms that explain the role of VP24 in host adaptation remain, however, to be defined (29). Interestingly, adaptation of Marburg viruses to rodents has not resulted in changes in VP24, but changes to VP40 have occurred. Seven amino acid changes accumulated in VP40 during adaptation of RAVV to mice, and one amino acid substitution was observed in VP40 after adaptation of MARV to guinea pigs, suggesting a possible role for VP40 in host tropism (19, 42, 43).

We demonstrate here that the VP40 from two distinct lineages of marburgvirus, RAVV and MARV, each efficiently inhibits IFN signaling in human cells. However, IFN-α/β-inducible STAT1 and STAT2 phosphorylation is not inhibited by either VP40 in murine cells. Interestingly, a mouse adapted RAVV VP40 is able to inhibit STAT1, STAT2 or Jak1 phosphorylation in both human and murine cells. We further demonstrate that maRAVV VP40 counteracts the antiviral effects of IFN in murine cells. Two amino acids are demonstrated to be responsible for the gain of the IFN signaling inhibitory function that occurred during the adaptation to mice. Finally, we demonstrate that VP40s from human isolates can bud from mouse cells as efficiently as the mouse-adapted VP40. These data suggest that VP40 antagonism of IFN signaling may be central to Marburg virus virulence in mice.

MATERIALS AND METHODS

Cell lines and viruses. Huh7 cells, Hepa1.6 cells, and STAT2$^{-/-}$ mouse embryo fibroblasts (MEFs) were maintained in Dulbecco modified Eagle medium (DMEM) supplemented with 5% fetal bovine serum and 10 mM HEPES (pH 7.5). A previously described Newcastle disease virus engineered to express green fluorescence protein (NDV-GFP) was propagated in 10-day-old embryonated chicken eggs (24).

Plasmids. PCR products corresponding to FLAG-tagged viral proteins of MARV (accession no. NC001608), RAVV (accession no. EU500827), maRAVV (accession no. EU500826), and the Langat virus (LGTV) of the *Flaviviridae* family (described in references 2 and 40) were cloned into the pCAGGS expression vector (22, 24). Human Jak1 (accession no. BAE02826) has been previously described (40), while mouse Jak1 (accession no. NP666257.2) was PCR amplified from a template and cloned with an N-terminal hemagglutinin (HA) tag into pCAGGS. Site-directed mutagenesis was performed by using a QuikChange XL II or Multi kit (Agilent Technologies, Santa Clara, CA).

Transfections. Hepa1.6 cells and STAT2$^{-/-}$ MEFs were transfected by using Lipofectamine 2000 (LF2K) at a ratio 1:3 with plasmid DNA (μg of DNA/μl of LF2K). The ratio for the transfection of Huh7 cells was 1:2.75. Cells were lysed with an IGEPAL lysis buffer (50 mM Tris [pH 8.0], 280 mM NaCl, 0.5% IGEPAL, 0.2 mM EDTA, 2 mM EGTA, 10% glycerol, and 1 mM dithiothreitol supplemented with protease inhibitor cocktail [Roche] and 0.1 mM Na_3VO_4) (31) for 30 min on ice and spun at 13,000 rpm in a refrigerated tabletop centrifuge for 1 min.

Cytokines. Universal type I IFN (a consensus IFN-α/β; PBL, Piscataway, NJ) was used at 1,000 IU/ml for 30 min in RPMI 1640 (Gibco) supplemented with 0.3% bovine serum albumin (BSA), unless otherwise specified.

Bioassay to monitor IFN-α/β-induced antiviral state. A total of 8×10^5 Hepa1.6 cells per well were cultured in six-well plates and transfected in triplicate with 3 μg of viral protein expression plasmid. At 24 h posttransfection, cells were infected with NDV-GFP at a multiplicity of infection (MOI) of 10 in a volume of 1 ml of 0.3% BSA in RPMI 1640 for 1 h, washed twice, and replaced with DMEM supplemented with 10% fetal bovine serum (FBS). At 15 h postinfection, the cells were treated with trypsin, washed twice with phosphate-buffered saline (PBS) supplemented with 5% FBS, and analyzed by fluorescence-activated cell sorting (FACS) using a Beckman Coulter Cytometer FC 500 (Brea, CA) for GFP fluorescence intensity.

Western blotting and ELISAs. For the detection of the overexpressed viral proteins, the anti-HA and anti-FLAG M2 (Sigma) antibodies were used at a 1:5,000 dilution in 1% nonfat dry milk in Tris-buffered saline (TBS; 20 mM Tris-HCl [pH 7.4]; 150 mM NaCl). As a loading control, anti-beta-tubulin (Sigma) antibody was used at a 1:10,000 dilution in 1% nonfat dry milk in TBS. Anti-GFP (Clontech, Mountain View, CA) was used at a 1:10,000 dilution in 1% nonfat dry milk in TBS. Phosphorylated STAT1 was detected with a phosphotyrosine specific antibody recognizing phospho-Y701 (BD Transduction Laboratories, San Jose, CA), and the total levels of STAT1 were detected with an antibody recognizing the STAT1 C terminus (BD Transduction Laboratories), diluted to 1:1,000 and 1:500, respectively, in 1% nonfat dry milk in TBS. Phosphorylated (pY689) STAT2 was detected with polyclonal antibodies (Millipore, Temecula, CA) diluted 1:500 in 5% nonfat dry milk and 0.2% Tween in TBS. Anti-pY1022/1023-Jak1 (Cell Signaling, Beverly, MA) and anti-total Jak1 (BD Transduction Laboratories) antibodies were used at a 1:500 dilution in TBS, 0.1% Tween and 5% BSA. For the detection of mouse IFN-β, a mouse interferon beta enzyme-linked immunosorbent assay (ELISA) kit (PBL Biomedical Laboratories) was used on supernatants of Hepa1.6 cells that had been transfected 36 h before and diluted 1:10, 1:100, and 1:1,000 in sample dilution buffer.

VLP budding assay. Hepa1.6 cells were transfected with 2 μg of expression plasmid. At 48 h posttransfection, cell culture supernatants were clarified by centrifugation at $200 \times g$ for 5 min and then pelleted through a 20% sucrose cushion in NTE buffer (100 mM NaCl, 10 mM Tris [pH 7.5], 1 mM EDTA [pH 8.0]) at $160,000 \times g$ for 2 h at 4°C. Supernatants were aspirated, and the pellets containing the VLPs were resuspended in NTE buffer. Cells were washed with PBS and lysed in radioimmunoprecipitation assay buffer (50 mM Tris [pH 7.4], 150 mM NaCl, 0.1% sodium dodecyl sulfate [SDS], 0.5% deoxycholate, 1% NP-40) supplemented with protease and phosphatase inhibitor cocktail (Roche). VLPs and lysates were analyzed by SDS-PAGE and visualized by Western blotting (7, 40).

Data and statistical analysis. The Student one-tailed *t* test was used to compare the means of continuous data using the GraphPad Prism statistical package.

RESULTS

The VP40 protein of RAVV inhibits IFN-α/β signaling in human but not mouse cells. Because VP40s from RAVV and MARV Musoke strain differ at 4 amino acid positions, the two proteins were compared for their inhibition of IFN-α/β signaling in both human and mouse cells. The human hepatoma cell line Huh7 was transfected with plasmids that express a human STAT1-GFP fusion and either the empty expression plasmid pCAGGS or plasmids that express either FLAG-tagged NS5 from Langat virus (LGTV NS5), a previously described inhibitor of IFN-induced Jak-STAT signaling (2), RAVV VP40, or MARV VP40. At 24 h posttransfection, the cells were treated with IFN-α/β and lysed 30 min later. The IFN-induced phosphorylation of STAT1-GFP was examined by Western blotting with a phospho-STAT1 specific antibody. Both RAVV and MARV VP40 inhibited the phosphorylation of STAT1-GFP (Fig. 1A). Note that the upper band corresponds to STAT1-GFP, while the lower band corresponds to endogenous STAT1 (Fig. 1A).

It was also of interest to assess VP40 function in mouse cells. In the mouse hepatoma cell line Hepa1.6, the positive control inhibitor, LGTV NS5, was able to completely inhibit STAT1-GFP phosphorylation. In contrast, neither MARV nor RAVV VP40 efficiently inhibited STAT1-GFP tyrosine phosphorylation (Fig. 1B), suggesting that these VP40s, which have not undergone mouse-adaptation, are relatively ineffective antagonists of the IFN-α/β response in mouse cells. During the course of experiments in Hepa1.6 cells, we noted a reproducible and significant level of STAT1 tyrosine phosphorylation in the absence of exogenous IFN-α/β (Fig. 1B). To determine

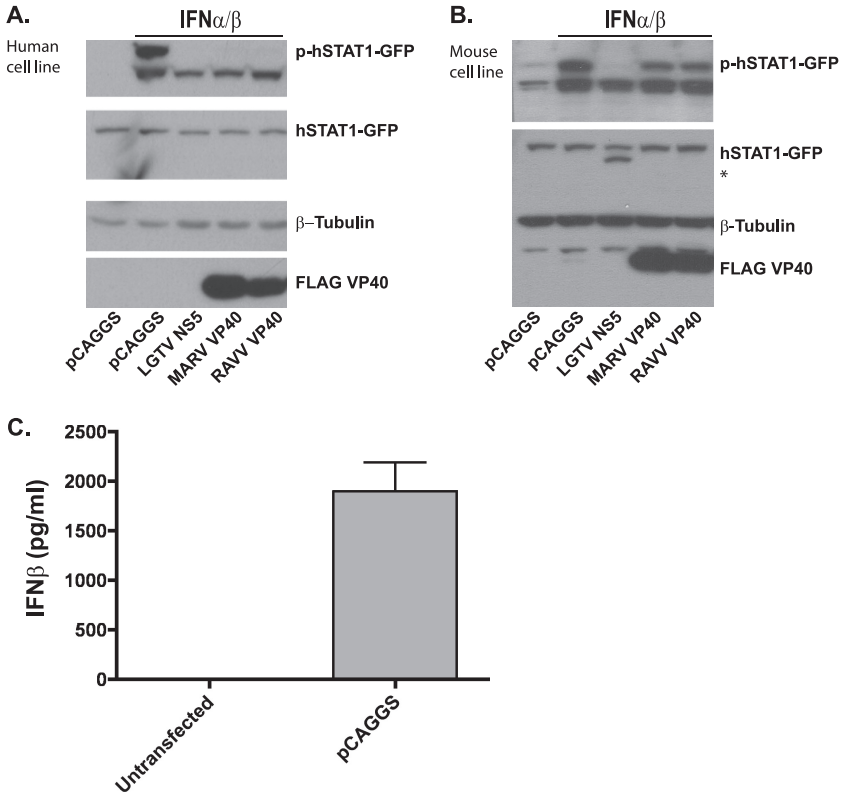

FIG. 1. The VP40 proteins of RAVV and MARV inhibit IFN-α/β signaling in human but not mouse cells. Huh7 (A) or Hepa1.6 (B) cells were transfected with hSTAT1-GFP expression plasmid and either empty vector (pCAGGS) or the indicated expression plasmids encoding FLAG-tagged viral proteins. At 24 h posttransfection, the cells were treated with IFN-α/β (1,000 U/ml) for 30 min and analyzed by Western blotting for STAT1 phosphorylation. The total levels of STAT1-GFP were evaluated with an anti-GFP antibody, an anti-β-tubulin blot served as a loading control, and anti-FLAG antibody was used to assess viral protein expression. The asterisk (*) indicates the band that corresponds to FLAG-tagged LGTV NS5. (C) Hepa1.6 cells were either left untransfected or were transfected with empty vector (pCAGGS). At 36 h after transfection, IFN-β was measured by ELISA.

whether this was due to transfection-induced IFN-α/β release, an ELISA was performed to detect mouse IFN-β in the supernatants of untransfected and empty vector (pCAGGS)-transfected Hepa1.6 cells. The Hepa1.6 cell supernatants contained approximately 2 ng of IFN-β/ml when transfected, while IFN-β in the supernatants from untransfected cells was below the level of detection (Fig. 1C). Despite this endogenous IFN-β production and the addition of IFN-β, the LGTV NS5 fully blocked STAT1-GFP phosphorylation (Fig. 1B).

Mouse adaptation of RAVV resulted in a VP40 with enhanced ability to suppress IFN-α/β signaling in mouse cells. The parental RAVV and the maRAVV VP40 proteins differ at 7 amino acid residues (Fig. 2A) (43). To determine whether these changes enhance the capacity of RAVV VP40 to inhibit IFN-α/β signaling in mouse cells, Hepa1.6 cells were transfected with STAT1-GFP and either empty vector (pCAGGS) or plasmids expressing LGTV NS5, MARV, RAVV, or mouse-adapted (ma) RAVV VP40. 30 min after IFN-α/β addition STAT1-GFP tyrosine phosphorylation was assessed. Whereas the parental MARV and RAVV VP40s only modestly reduced STAT1 phosphorylation, the maRAVV VP40 was a highly effective inhibitor, reducing STAT1 phosphorylation to levels seen with the LGTV NS5 positive control (Fig. 2B). To determine whether maRAVV VP40 was also functional in human cells, Huh7 cells were transfected as in Fig. 2B. maRAVV VP40 was able to inhibit IFN-α/β-induced STAT1 phosphorylation in human cells as well as in murine cells (Fig. 2C). In human cells MARV VP40 expression inhibits Jak1 function and therefore also causes a loss of both STAT1 and STAT2 tyrosine phosphorylation in response to IFN-α/β (40). To determine whether maVP40 can also inhibit IFN-α/β induced STAT2 phosphorylation in mouse cells, STAT2 deficient mouse embryonic fibroblasts ($STAT2^{-/-}$ MEFs) were transfected with a FLAG-tagged mouse STAT2 expression plasmid and with plasmids expressing LGTV NS5, MARV VP40, RAVV VP40, or maRAVV VP40. After addition of IFN-α/β, both LGTV NS5 and maRAVV VP40 completely abrogated STAT2 phosphorylation, whereas the parental VP40s again were poor inhibitors of IFN-α/β signaling in the mouse cells (Fig. 2D). These data demonstrate that although neither the nonadapted MARV nor the RAVV VP40s effectively inhibit IFN-α/β signaling in mouse cells, RAVV VP40 acquired this capability during mouse adaptation.

maRAVV VP40 inhibits the phosphorylation of overexpressed Jak1 in murine and human cells. Overexpression of Janus kinases leads to the tyrosine phosphorylation of the overexpressed kinase and to the tyrosine phosphorylation of STAT proteins (27, 40). Previously, MARV VP40 was demonstrated to inhibit the tyrosine phosphorylation of Jak1 and STATs 1, 2, and

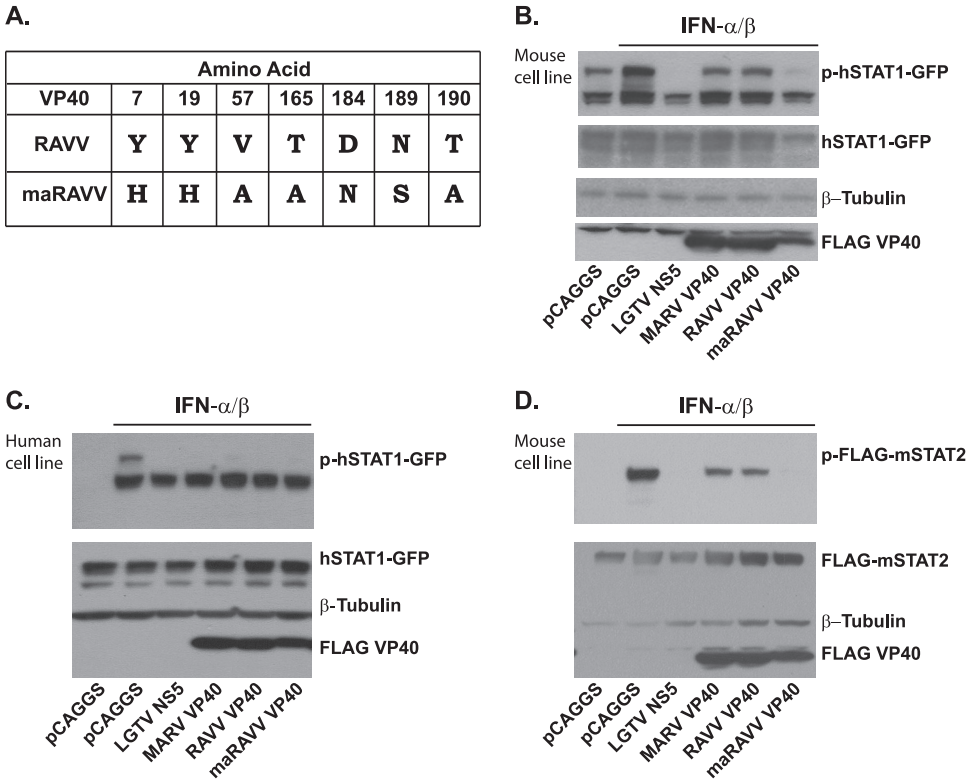

FIG. 2. Mouse-adapted RAVV VP40 exhibits enhanced ability to suppress IFN-α/β signaling in mouse cells. (A) The seven amino acid positions at which RAVV VP40 and maRAVV VP40 differ are indicated. Hepa1.6 (B) or Huh7 (C) cells were transfected with hSTAT1-GFP plasmid and empty vector (pCAGGS) or the indicated expression plasmids for FLAG-tagged viral proteins. At 24 h posttransfection, cells were treated with IFN-α/β (1,000 U/ml for 30 min) and analyzed for STAT1 phosphorylation. Total levels of STAT1-GFP were evaluated with an anti-STAT1, β-tubulin was used as a loading control, and anti-FLAG was used to assess protein expression. (D) STAT2$^{-/-}$ MEFs were transfected with FLAG-mSTAT2 plasmid and the indicated plasmids. At 48 h posttransfection, the cells were treated with IFN-α/β (1,000 U/ml) for 30 min and analyzed by Western blotting for FLAG-mSTAT2 phosphorylation. Anti-FLAG antibody was used to evaluate the total levels of FLAG-mSTAT2 and viral protein expression, while anti-β-tubulin antibody was used as a loading control.

3 in Jak1-overexpressing Huh7 cells (40). To determine whether maRAVV VP40 can inhibit the phosphorylation of Jak1 and of STAT proteins in Jak1 overexpressing mouse cells, Hepa1.6 cells were transfected with either mouse or human Jak1 and with empty vector or plasmids expressing LGTV NS5, MARV, RAVV, or maRAVV VP40. maRAVV VP40 inhibited the tyrosine phosphorylation of both human and mouse Jak1, as well as the Jak1-dependent phosphorylation of endogenous STAT1 in these cells (Fig. 3A). To determine whether the VP40s were also able to inhibit Jak1 and STAT1 phosphorylation in human cells, Huh7 cells were transfected in a similar manner as described above. Each of the three VP40s inhibited the phosphorylation of both human and mouse Jak1, as well as that of endogenous STAT1 in the human cells (Fig. 3B). The ability of maRAVV VP40 to inhibit human Jak1 in mouse cells coupled with the fact that the nonadapted VP40s inhibit mouse Jak1 in human cells suggests that VP40 does not simply recognize Jak1. Rather, another factor in mouse cells must contribute to the inhibition of IFN-α/β signaling in mouse cells.

maRAVV VP40 can counteract the antiviral effects of IFN in murine cells. To assess the impact of VP40 expression on the antiviral effects of IFN-α/β in mouse cells, Hepa1.6 cells were transfected with expression plasmids for LGTV NS5, MARV VP40, RAVV VP40, and maRAVV VP40. As shown in Fig. 1D, transfection of Hepa1.6 cells induces IFN-β. This is sufficient to induce an antiviral state in these cells such that when empty vector transfected cells were infected with a Newcastle disease virus that expresses GFP (NDV-GFP) and analyzed by FACS for GFP expression at 15 h postinfection, virus replication and GFP expression was greatly suppressed relative to untransfected cells (Fig. 4A). That the suppression is mediated by IFN-α/β is supported by the fact that expression of a known inhibitor of IFN signaling, LGTV NS5, rescues NDV-GFP replication (Fig. 4A). By comparison, the nonadapted MARV and RAVV VP40-transfected cells exhibited GFP expression levels comparable to that seen in the empty vector-transfected cells, whereas maRAVV VP40 restored GFP expression to levels seen with LGTV NS5 (Fig. 4A). Figure 4B presents the means of three independent experiments measuring the mean green fluorescence intensity. Expression of maRAVV VP40 in mouse cells significantly increases virus replication in the presence of IFN-α/β, relative to the nonadapted RAVV VP40. Therefore, mouse adaptation allows VP40 to block the antiviral effects of IFN-α/β in mouse cells.

The identity of residues 57 and 165 is critical for VP40 inhibition of IFN signaling in mouse cells. To identify the residues that are important for the inhibition of IFN signaling in mouse cells, point mutations were introduced in the

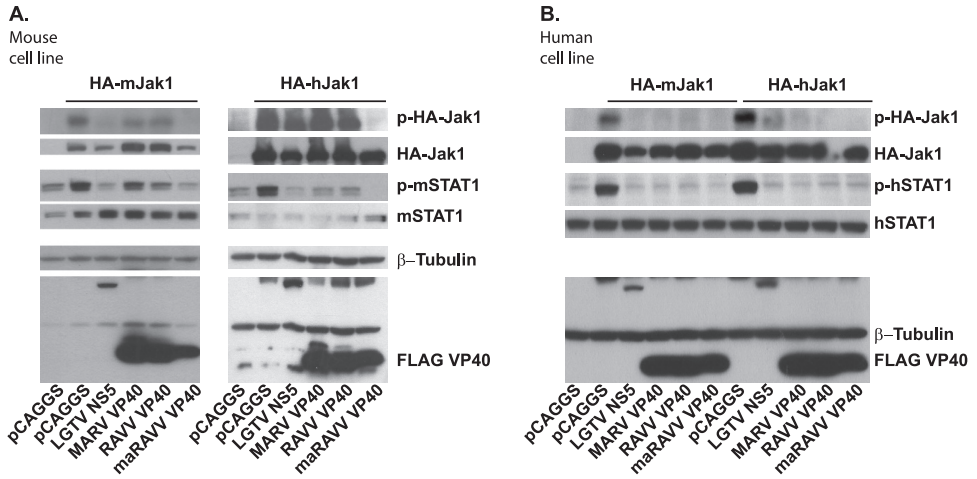

FIG. 3. maRAVV VP40 inhibits the phosphorylation of overexpressed Jak1 in both murine and human cells. Hepa1.6 (A) and Huh7 (B) cells were transfected with either human or mouse HA-tagged Jak1 and the indicated expression plasmids. At 24 h posttransfection, the phosphorylation of Jak1 and the Jak1-dependent phosphorylation of endogenous STAT1 was evaluated. Anti-HA, anti-FLAG, and anti-STAT1 antibodies were used to evaluate the protein levels by Western blotting, while β-tubulin was used as a loading control.

maRAVV VP40 background, such that a given residue was mutated to the corresponding amino acid in the nonadapted RAVV VP40. Specifically, the following mutants were constructed in the maRAVV VP40 cDNA: H7Y, H19Y, A57V, A165T, N184D, and an S189N/A190T double mutant. The mutant VP40s and appropriate controls were cotransfected with FLAG-tagged mouse STAT2 into STAT2$^{-/-}$ MEFs, and at 48 h posttransfection the cells were treated with IFN-α/β for 30 min and then analyzed by Western blotting for STAT2 phosphorylation (Fig. 5A). All mutants except A57V and A165T inhibited STAT2 phosphorylation as efficiently as maRAVV VP40 did. The single amino acid substitution mutants A57V or A165T or a double mutant (A57V/A156T) each lost the ability to inhibit STAT2 phosphorylation in mouse cells (Fig. 5A). To examine the biological significance of the mutations, an IFN bioassay was performed in Hepa1.6 cells. The assay is analogous to that described above but included the mutant maVP40s. In this experiment, maRAVV VP40 was able to rescue viral replication such that GFP expression reached 30% of the untransfected control, whereas the mutations A57V and A165T, either alone or combined, resulted in a significant reduction in GFP expression (Fig. 5B). To determine whether the introduced mutations were generally deleterious to VP40 function, Huh7 cells were transfected with a human STAT1-GFP plasmid along with the expression plasmids tested in Fig. 5A and B. 30 min after IFN-α/β addition, STAT1-GFP tyrosine phosphorylation was assessed. All of the mutants, as well as the wild-type nonadapted and mouse-adapted VP40s, inhibited STAT1 phosphorylation, indicating that the mutants are functional in human cells (Fig. 5C). These data demonstrate that the identities of residues 57

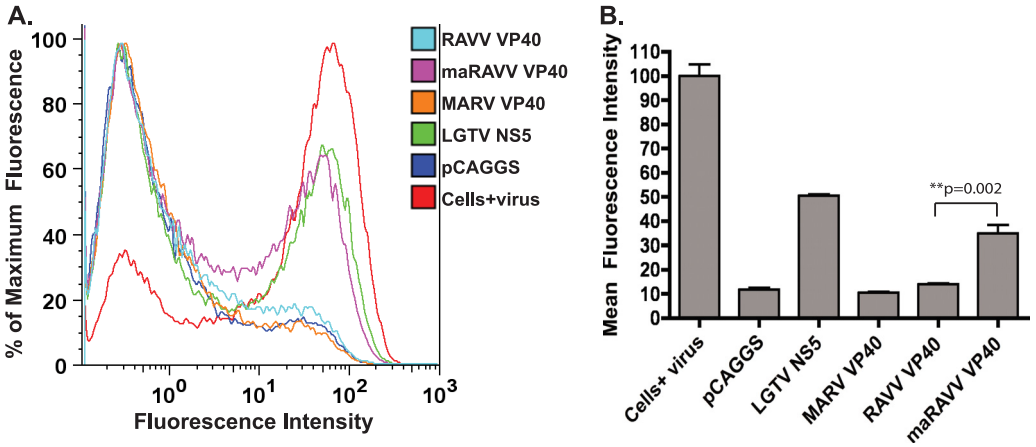

FIG. 4. maRAVV VP40 can counteract the antiviral effects of IFN in murine cells. Hepa1.6 cells were transfected with the indicated expression plasmids. At 24 h posttransfection, the cells were infected with NDV-GFP at an MOI of 10. (A) At 15 h postinfection, the cells were analyzed by FACS, and the fluorescence intensity of the virus-expressed GFP from representative samples is shown. (B) Bars represent the mean fluorescence intensity ($n = 3$), and error bars represent the standard deviations. Western blots against β-tubulin and FLAG were used as a loading control and to confirm equal expression of viral proteins (data not shown).

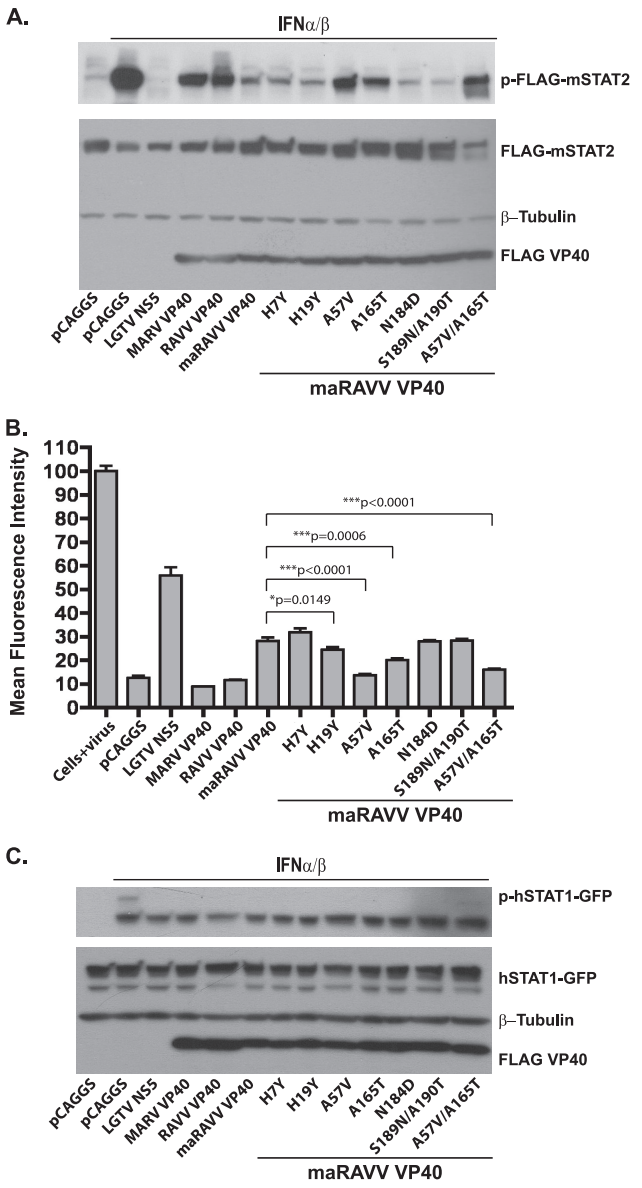

FIG. 5. Amino acid changes A57V or A165T render maRAVV unable to inhibit signaling in mouse cells. (A) STAT2$^{-/-}$ MEFs were transfected with FLAG-mSTAT2 and the indicated expression plasmids for wild-type, single amino acid mutants or double amino acid mutants of FLAG-tagged maRAVV VP40 as indicated. At 48 h posttransfection, the cells were treated with IFN-α/β (1,000 U/ml) for 30 min and analyzed by Western blotting for FLAG-mSTAT2 phosphorylation. Anti-FLAG antibody was used to evaluate the total levels of FLAG-mSTAT2 and viral protein expression, while β-tubulin levels served as a loading control. (B) Hepa1.6 cells were transfected with the indicated plasmids and, at 24 h posttransfection, the cells were infected with NDV-GFP at an MOI of 10. At 15 h postinfection, the cells were analyzed by FACS, and the mean fluorescence intensity ($n = 3$) corresponding to virus growth is shown, with error bars representing the standard deviations. Western blots for β-tubulin and FLAG were used as a loading control and to confirm equal expression of viral proteins (data not shown). (C) Huh7 cells were transfected with hSTAT1-GFP expression plasmid and empty vector (pCAGGS) or the indicated plasmids expressing FLAG-tagged viral proteins. At 24 h posttransfection, the cells were treated with IFN-α/β (1,000 U/ml) for 30 min and analyzed by Western blotting for STAT1 phosphorylation. Total levels of STAT1-GFP were evaluated with anti-STAT1 antibody, β-tubulin levels served as a loading control, and anti-FLAG antibody was used to assess viral protein expression.

and 165 are critical for VP40 inhibition of IFN signaling in mouse cells.

As a complementary approach, point mutations were introduced into the nonadapted version of RAVV VP40 in order to identify amino acid changes sufficient to confer the inhibitory function in mouse cells. FLAG-tagged mouse STAT2 was cotransfected into STAT2$^{-/-}$ MEFs with empty expression plasmid, plasmids for FLAG-tagged LGTV NS5 and wild-type or mutant VP40s. Examination of FLAG-STAT2 phosphorylation 30 min after IFN-α/β treatment indicated that the combination of V57A and T165A mutations permits RAVV VP40 to block IFN-α/β signaling comparably to the maRAVV VP40 (Fig. 6A). In the bioassay, the individual RAVV VP40 mutants V57A and T165A modestly rescued viral replication, and RAVV VP40 V57A/T165A restored virus replication to levels higher than was seen with maRAVV VP40 (Fig. 6B).

To determine whether the same residues influence the function of the MARV VP40, MARV VP40 mutants V57A, T165A, and V57A/T165A were generated and tested for inhibition of IFN-α/β signaling in mouse cells using the same approach as that described for Fig. 6A and B. Again, the V57A/T165A double mutant was able to inhibit STAT2 phosphorylation comparably to maRAVV VP40 (Fig. 6C) and was able to restore virus replication levels higher than that of maRAVV VP40 (Fig. 6D).

Mutations acquired during mouse adaptation do not influence RAVV VP40 budding in mouse cells. The ability of VP40 to bud from cells is thought to be critical for virus release. It was therefore of interest to determine whether any of the mutations acquired during mouse adaptation affect the ability of VP40 to bud from Hepa1.6 cells. Of particular interest was the change Y19H, which is part of the previously described late domain (43). Included in this experiment were MARV VP40, RAVV VP40, and maRAVV VP40. To directly assess the impact of changes at the late domain, RAVV VP40-Y19H and maRAVV VP40-H19Y were also tested. Finally, the mutants at residues 57 and 165, which exhibited gain or loss of function in the IFN-α/β signaling assays were examined. Each expression plasmid was transfected into Hepa1.6 cells. GFP was also included as a control protein that does not bud from cells. At 48 h posttransfection, the VLPs present in the supernatants from the transfected cells were pelleted through a 20% sucrose cushion, and the pellets were examined by Western blotting to detect FLAG-VP40. All of the constructs yielded comparable levels of budded VP40, with the Y19H mutant showing only a very modest 2-fold decrease, as determined by densitometry of the blots, relative to the wild-type VP40. Therefore, the changes that occurred during mouse-adaptation of VP40 do not detectably affect RAVV VP40 budding in Hepa1.6 cells (Fig. 7).

DISCUSSION

An understanding of the determinants of virulence in different host species is fundamental to our understanding of the zoonotic nature of filoviruses. *Rousettus aegyptiacus* bats have been implicated as reservoirs of Marburg viruses (37, 38). In the laboratory, examining the adaptation of these viruses to rodents may provide clues to viral and host factors that determine the outcome of these infections. Experimental infections

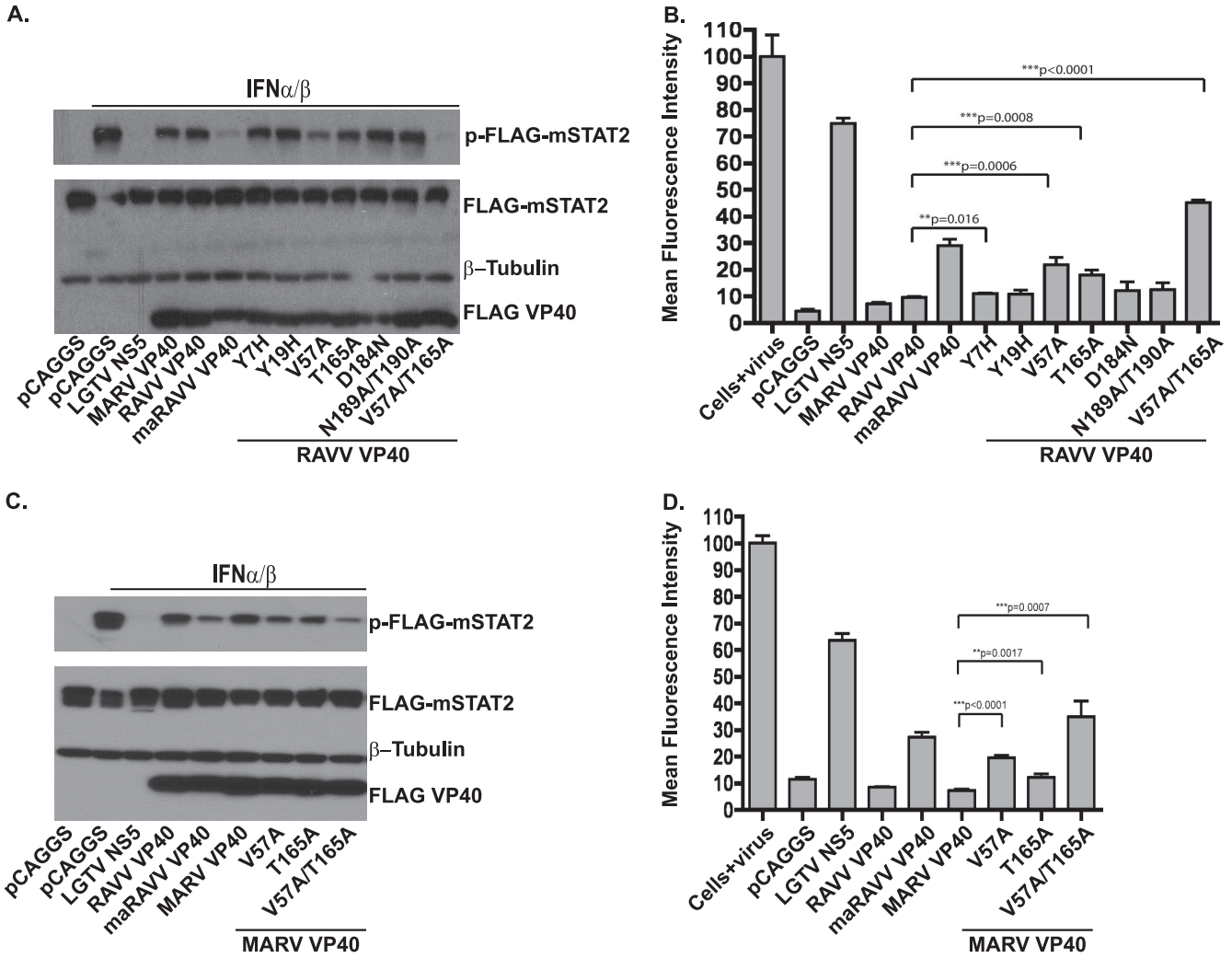

FIG. 6. The combined changes V57A and T165A render the RAVV and MARV VP40s able to antagonize IFN-α/β in mouse cells. STAT2$^{-/-}$ MEFs were transfected with FLAG-mSTAT2 expression plasmid and empty vector or expression plasmids for the indicated wild-type, single amino acid mutant, or double amino acid FLAG-tagged RAVV VP40s (A) or MARV VP40s (C) as indicated. At 48 h posttransfection, the cells were treated with IFN-α/β (1,000 U/ml for 30 min) and analyzed by Western blotting for FLAG-mSTAT2 phosphorylation. Anti-FLAG antibody was used to evaluate the total levels of FLAG-mSTAT2 and viral protein expression, while β-tubulin levels served as a loading control. Hepa1.6 cells were transfected with expression plasmids for the RAVV VP40 (B) or MARV VP40 (D) constructs and, 24 h posttransfection, the cells were infected with NDV-GFP at an MOI of 10. At 15 h postinfection, the cells were analyzed by FACS. The mean fluorescence intensity ($n = 3$) from virus-expressed GFP is shown, with error bars representing the standard deviations. Western blots against β-tubulin and FLAG were used as a loading control and to confirm equal expression of proteins (not shown).

with filovirus isolates that cause severe disease in humans do not typically result in disease in rodents. Experiments in mice previously demonstrated a role for the host IFN-α/β responses in the resistance of this species to lethal infection by nonadapted filoviruses. For example, intraperitoneal infection of adult wild-type mice did not result in lethal infection with nonadapted Marburg viruses or EBOVs. In contrast, IFN receptor knockout mice succumbed to infection with nonadapted Marburg viruses or EBOVs. Administration to animals of anti-IFN-α/β antibodies also potentiates filovirus disease (4). Further, adaptation of Marburg viruses or EBOVs overcomes their inability to cause disease in IFN-competent animals (5, 9, 19, 41–43). These observations implicate the host IFN-α/β response in host restriction of filoviruses, at least in mice. However, the molecular basis by which adaptation allows disease to occur in IFN-competent animals remains incompletely defined.

The present study demonstrates that both the nonadapted MARV VP40 and the VP40 of nonadapted RAVV, a marburgvirus from a different clade than MARV, inhibit IFN-α/β signaling and prevent signaling in Jak1-overexpressing human cells. These observations are consistent with the prior observation that MARV infection or expression of MARV VP40 inhibits Jak1-dependent signaling in primate cells (40). This results in a loss of cellular responsiveness to IFN-α/β or IFN-γ, mimicking the phenotype of Jak1-knockout cells. Thus, the MARV-infected or VP40-expressing cells exhibited a general loss of tyrosine phosphorylation of Jak tyrosine kinases and STAT proteins after the addition of IFN-α/β or IFN-γ to cells. These cells also exhibited resistance to the antiviral effects of

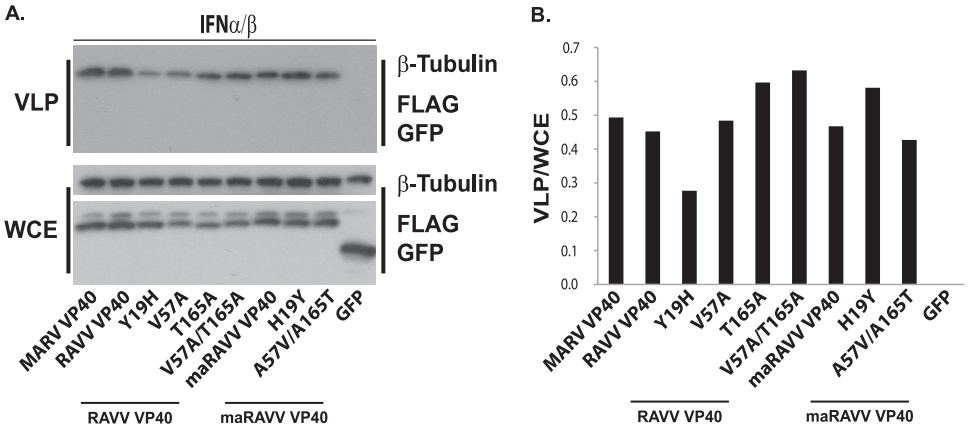

FIG. 7. Mutations acquired during mouse-adaptation do not influence RAVV VP40 budding in mouse cells. (A) Hepa1.6 cells were transfected with the indicated plasmids encoding FLAG-tagged wild-type or mutant RAVV VP40s. At 8 h posttransfection, 1,000 U of IFN-α/β/ml was added with fresh medium to the cells. After 40 h, the supernatants were harvested, and VLPs were purified through a sucrose cushion. Cells were lysed and examined together with the VLPs for protein expression levels (WCE, whole-cell extract). Anti-FLAG, anti-GFP, and anti-β-tubulin antibodies were used in both the WCE and the VLP blot. (B) Bands from panel A were quantified by using NIH ImageJ, and the ratio of VLP intensity to the WCE intensity was graphed after subtracting the value obtained for GFP.

IFN-α/β. When Jak family tyrosine kinases are overexpressed in Huh7 cells, the overexpressed kinase becomes tyrosine phosphorylated, as do cellular STAT proteins. In support of the view that Jak1 is a critical and specific target of VP40, expression of either RAVV or MARV VP40 inhibits the tyrosine phosphorylation of Jak1 and STAT proteins in Jak1-overexpressing human cells (40) (Fig. 3).

Notably, neither MARV nor RAVV VP40 could efficiently inhibit IFN-α/β signaling in the mouse cells tested (Fig. 1). Although a modest reduction in STAT1 or STAT2 phosphorylation could be seen in VP40-expressing mouse cells, relative to empty vector-transfected control cells, this inhibition was not sufficient to counteract the antiviral effects of IFN (Fig. 4). Strikingly, however, adaptation of RAVV to mice resulted in a VP40 fully capable of inhibiting IFN signaling and blocking the antiviral effects of IFN-β in mouse cells (Fig. 2 and 4). Moreover, maRAVV VP40 was able to inhibit the phosphorylation of either mouse or human Jak1 and STAT1 in human and mouse cells, while the nonadapted VP40s inhibited the phosphorylation of human Jak1 and mouse Jak1 in human cells but not in mouse cells (Fig. 3). These observations are consistent with a model where VP40 inhibition of Jak1 requires an additional host factor(s) to carry out its inhibitory function.

Given that the mouse-adapted RAVV exhibits increased virulence in mice, relative to the parental strain from which it was derived, the enhanced IFN antagonist function is consistent with a role for VP40 IFN antagonist function in mouse pathogenesis. Whether the mouse-adaptive changes in VP40 are sufficient for enhanced virulence in the absence of other changes remains to be determined. It is intriguing that the mouse-adapted RAVV also accumulated several amino acid changes in its VP35 protein. In EBOV, VP35 has been demonstrated to inhibit the production of IFN-α/β by antagonizing the RIG-I signaling pathway (6, 17). Whether these VP35 changes influence its function in mouse cells is therefore of interest.

Of the 7 amino acid changes that accumulated in RAVV VP40 during mouse adaptation, 2 residues (V57 and T165 in the nonadapted RAVV VP40) proved to be critical for IFN antagonist function in mouse cells. This was evidenced by the gain of IFN antagonist function in mouse cells when only these two residues were mutated to alanine in the context of an otherwise nonadapted RAVV VP40. Both changes appear to be required for full activity, although very modest increases in inhibitory function were seen with individual changes at these residues (e.g., Fig. 5). Also, the individual mutation of either residue back to V57 or T165 in the context of the mouse-adapted VP40 was sufficient to abrogate function in mouse cells. When the V57A/T165A mutations were examined in the context of the MARV VP40, this also conferred the ability to inhibit IFN signaling in mouse cells, further emphasizing the importance of these residues. A working hypothesis would be that these residues allow VP40 to interact with an unidentified factor in mouse cells that mediates inhibition of Jak1. How the very conservative valine to alanine change at residue 57 dramatically affects function remains to be determined. It is noteworthy that VP40s with an alanine at this position reproducibly exhibit slightly retarded migration on SDS-PAGE, suggesting a possible structural change or posttranslational modification of the viral protein.

Expression of VP40 alone is able to drive the formation of VLPs that bud from the cell membrane. Filoviral VP40s have well-characterized late domains important for the budding process: ZEBOV VP40 possesses two late domains, a PTAP motif and an overlapping PPXY motif, which mediate interaction with Tsg101, Nedd4, and Rsp5. MARV VP40 possesses a single $_{13}$PPPY$_{16}$ motif that allows interaction with Tsg101, although it has been proposed that NP can also recruit Tsg101 to sites of MARV VP40 budding (8, 13, 23, 35, 39). Our previous study suggested that the two functions of MARV VP40—IFN signaling antagonism and VLP formation—are independent (40). During the adaptation of RAVV, one of the seven amino acids that were changed was the tyrosine at position 16 (43). This particular amino acid has been shown to be involved in interaction with Tsg101 (39). However, in mouse cells, change of this amino acid to a histidine only reduced the

ability of the protein to bud by 2-fold (Fig. 7). None of the other mutations that are involved in IFN antagonism in mouse cells altered the protein's ability to bud. Therefore, our data suggest that the budding function of RAVV VP40 did not need to adapt to the mouse.

The present study identifies a specific molecular function that changed during RAVV adaptation to mice. The host factor(s) that interact with VP40 to mediate its IFN antagonist function should shed light upon its mechanism of action, and the availability of VP40s that do or do not function in mouse cells provides a useful system that may allow the identification of these critical host factors. Additional studies will be required to define the contribution of these changes to virulence in mice and determine the contribution to host adaptation of other changes in VP40.

ACKNOWLEDGMENTS

This study was supported by NIH grants AI059536 and AI057158 (Northeast Biodefense Center-Lipkin) to C.F.B.

We thank Adolfo García-Sastre (Mount Sinai School of Medicine) for the FLAG-mSTAT2 construct, Sonja Best (National Institute for Allergy and Infectious Diseases) for the LGTV NS5 construct, Lu-Hai Wang (Mount Sinai School of Medicine and National Health Research Institutes, Taiwan) for the mouse Jak1 construct, Analisa DiFeo (Mount Sinai School of Medicine) for the Huh7 cell line, Matthew Evans (Mount Sinai School of Medicine) for the Hepa1.6 line, and Benjamin tenOever (Mount Sinai School of Medicine) for the STAT2$^{-/-}$ MEFs.

REFERENCES

1. **Basler, C. F., et al.** 2000. The Ebola virus VP35 protein functions as a type I IFN antagonist. Proc. Natl. Acad. Sci. U. S. A. **97:**12289–12294.
2. **Best, S. M., et al.** 2005. Inhibition of interferon-stimulated JAK-STAT signaling by a tick-borne flavivirus and identification of NS5 as an interferon antagonist. J. Virol. **79:**12828–12839.
3. **Biron, C. A., L. P. Cousens, M. C. Ruzek, H. C. Su, and T. P. Salazar-Mather.** 1998. Early cytokine responses to viral infections and their roles in shaping endogenous cellular immunity. Adv. Exp. Med. Biol. **452:**143–149.
4. **Bray, M.** 2001. The role of the type I interferon response in the resistance of mice to filovirus infection. J. Gen. Virol. **82:**1365–1373.
5. **Bray, M., K. Davis, T. Geisbert, C. Schmaljohn, and J. Huggins.** 1998. A mouse model for evaluation of prophylaxis and therapy of Ebola hemorrhagic fever. J. Infect. Dis. **178:**651–661.
6. **Cardenas, W. B., et al.** 2006. Ebola virus VP35 protein binds double-stranded RNA and inhibits alpha/beta interferon production induced by RIG-I signaling. J. Virol. **80:**5168–5178.
7. **Ciancanelli, M. J., and C. F. Basler.** 2006. Mutation of YMYL in the Nipah virus matrix protein abrogates budding and alters subcellular localization. J. Virol. **80:**12070–12078.
8. **Dolnik, O., L. Kolesnikova, L. Stevermann, and S. Becker.** 2010. Tsg101 is recruited by a late domain of the nucleocapsid protein to support budding of Marburg virus-like particles. J. Virol. **84:**7847–7856.
9. **Ebihara, H., et al.** 2006. Molecular determinants of Ebola virus virulence in mice. PLoS Pathog. **2:**e73.
10. **Fields, B. N., et al. (ed.).** 2007. Fields virology, 5th ed. Lippincott-Raven Publishers, Philadelphia, PA.
11. **Guschin, D., et al.** 1995. A major role for the protein tyrosine kinase JAK1 in the JAK/STAT signal transduction pathway in response to interleukin-6. EMBO J. **14:**1421–1429.
12. **Hartman, A. L., J. S. Towner, and S. T. Nichol.** 2004. A C-terminal basic amino acid motif of Zaire ebolavirus VP35 is essential for type I interferon antagonism and displays high identity with the RNA-binding domain of another interferon antagonist, the NS1 protein of influenza A virus. Virology **328:**177–184.
13. **Harty, R. N., M. E. Brown, G. Wang, J. Huibregtse, and F. P. Hayes.** 2000. A PPxY motif within the VP40 protein of Ebola virus interacts physically and functionally with a ubiquitin ligase: implications for filovirus budding. Proc. Natl. Acad. Sci. U. S. A. **97:**13871–13876.
14. **Johnson, E. D., et al.** 1996. Characterization of a new Marburg virus isolated from a 1987 fatal case in Kenya. Arch. Virol. Suppl. **11:**101–114.
15. **Kolesnikova, L., E. Ryabchikova, A. Shestopalov, and S. Becker.** 2007. Basolateral budding of Marburg virus: VP40 retargets viral glycoprotein GP to the basolateral surface. J. Infect. Dis. **196**(Suppl. 2)**:**S232–S236.
16. **Kolesnikova, L., et al.** 2009. Vacuolar protein sorting pathway contributes to the release of Marburg virus. J. Virol. **83:**2327–2337.
17. **Leung, D. W., et al.** 2010. Structural basis for dsRNA recognition and interferon antagonism by Ebola VP35. Nat. Struct. Mol. Biol. **17:**165–172.
18. **Liu, Y., et al.** 2010. Conserved motifs within Ebola and Marburg virus VP40 proteins are important for stability, localization, and subsequent budding of virus-like particles. J. Virol. **84:**2294–2303.
19. **Lofts, L. L., M. S. Ibrahim, D. L. Negley, M. C. Hevey, and A. L. Schmaljohn.** 2007. Genomic differences between guinea pig lethal and nonlethal Marburg virus variants. J. Infect. Dis. **196**(Suppl. 2)**:**S305–S312.
20. **Mateo, M., S. P. Reid, L. W. Leung, C. F. Basler, and V. E. Volchkov.** 2010. Ebolavirus VP24 binding to karyopherins is required for inhibition of interferon signaling. J. Virol. **84:**1169–1175.
21. **Muller, M., et al.** 1993. The protein tyrosine kinase JAK1 complements defects in interferon-alpha/beta and -gamma signal transduction. Nature **366:**129–135.
22. **Niwa, H., K. Yamamura, and J. Miyazaki.** 1991. Efficient selection for high-expression transfectants with a novel eukaryotic vector. Gene **108:**193–199.
23. **Noda, T., et al.** 2006. Assembly and budding of ebolavirus. PLoS Pathog. **2:**e99.
24. **Park, M. S., et al.** 2003. Newcastle disease virus (NDV)-based assay demonstrates interferon-antagonist activity for the NDV V protein and the Nipah virus V, W, and C proteins. J. Virol. **77:**1501–1511.
25. **Platanias, L. C.** 2005. Mechanisms of type-I- and type-II-interferon-mediated signaling. Nat. Rev. Immunol. **5:**375–386.
26. **Prins, K. C., et al.** 2010. Mutations abrogating VP35 interaction with double-stranded RNA render Ebola virus avirulent in guinea pigs. J. Virol. **84:**3004–3015.
27. **Quelle, F. W., et al.** 1995. Phosphorylation and activation of the DNA-binding activity of purified Stat1 by the Janus protein-tyrosine kinases and the epidermal growth factor receptor. J. Biol. Chem. **270:**20775–20780.
28. **Reid, S. P., et al.** 2006. Ebola virus VP24 binds karyopherin alpha1 and blocks STAT1 nuclear accumulation. J. Virol. **80:**5156–5167.
29. **Reid, S. P., C. Valmas, O. Martinez, F. M. Sanchez, and C. F. Basler.** 2007. Ebola virus VP24 proteins inhibit the interaction of NPI-1 subfamily karyopherin alpha proteins with activated STAT1. J. Virol. **81:**13469–13477.
30. **Rodig, S. J., et al.** 1998. Disruption of the Jak1 gene demonstrates obligatory and nonredundant roles of the Jaks in cytokine-induced biologic responses. Cell **93:**373–383.
31. **Rodriguez, J. J., J. P. Parisien, and C. M. Horvath.** 2002. Nipah virus V protein evades alpha and gamma interferons by preventing STAT1 and STAT2 activation and nuclear accumulation. J. Virol. **76:**11476–11483.
32. **Ruigrok, R. W., et al.** 2000. Structural characterization and membrane binding properties of the matrix protein VP40 of Ebola virus. J. Mol. Biol. **300:**103–112.
33. **Sanchez, A., et al.** 1998. Variation in the glycoprotein and VP35 genes of Marburg virus strains. Virology **240:**138–146.
34. **Swenson, D. L., et al.** 2004. Generation of Marburg virus-like particles by coexpression of glycoprotein and matrix protein. FEMS Immunol. Med. Microbiol. **40:**27–31.
35. **Timmins, J., et al.** 2003. Ebola virus matrix protein VP40 interaction with human cellular factors Tsg101 and Nedd4. J. Mol. Biol. **326:**493–502.
36. **Tough, D. F.** 2004. Type I interferon as a link between innate and adaptive immunity through dendritic cell stimulation. Leuk. Lymphoma **45:**257–264.
37. **Towner, J. S., et al.** 2009. Isolation of genetically diverse Marburg viruses from Egyptian fruit bats. PLoS Pathog. **5:**e1000536.
38. **Towner, J. S., et al.** 2007. Marburg virus infection detected in a common African bat. PLoS One **2:**e764.
39. **Urata, S., et al.** 2007. Interaction of Tsg101 with Marburg virus VP40 depends on the PPPY motif, but not the PT/SAP motif as in the case of Ebola virus, and Tsg101 plays a critical role in the budding of Marburg virus-like particles induced by VP40, NP, and GP. J. Virol. **81:**4895–4899.
40. **Valmas, C., et al.** 2010. Marburg virus evades interferon responses by a mechanism distinct from Ebola virus. PLoS Pathog. **6:**e1000721.
41. **Volchkov, V. E., A. A. Chepurnov, V. A. Volchkova, V. A. Ternovoj, and H. D. Klenk.** 2000. Molecular characterization of guinea pig-adapted variants of Ebola virus. Virology **277:**147–155.
42. **Warfield, K. L., et al.** 2007. Development of a model for marburgvirus based on severe-combined immunodeficiency mice. Virol. J. **4:**108.
43. **Warfield, K. L., et al.** 2009. Development and characterization of a mouse model for Marburg hemorrhagic fever. J. Virol. **83:**6404–6415.
44. **Yang, C. H., A. Murti, W. J. Valentine, Z. Du, and L. M. Pfeffer.** 2005. Interferon alpha activates NF-κB in JAK1-deficient cells through a TYK2-dependent pathway. J. Biol. Chem. **280:**25849–25853.